CHEMISTRY OF MATERIALS
Communication

Chem. Mater. **2010,** *22,* 1949–1951 1949
DOI:10.1021/cm9038472

Effect of Carbon Incorporation on the Microstructure of BC_xN ($x = 0.25$, 1, and 4) Ternary Solid Solutions Studied by Transmission Electron Microscopy

I. Caretti,* R. Torres, R. Gago, A. R. Landa-Cánovas, and I. Jiménez

Instituto de Ciencia de Materiales de Madrid (ICMM-CSIC), Campus de Cantoblanco, 28049 Madrid, Spain

Received December 24, 2009
Revised Manuscript Received February 23, 2010

The family of boron−carbon−nitrogen (B−C−N) compounds is characterized by a rich compositional and structural diversity. Accordingly, a great variety of compounds in elemental, binary, or ternary form with different physicochemical properties coexist within the B−C−N compositional diagram (see Figure 1). In general, the most representative structural phases of the B−C−N system are: (i) hexagonal, found in graphite and *h*-BN; (ii) cubic, such as diamond or *c*-BN; (iii) icosahedral units, distinctive of B and B_4C; and (iv) amorphous, with different sp^3/sp^2 ratios (e.g., a-C and ta-C). Recently, the structural B−C−N map has been considerably expanded through the possibility of synthesizing a multiplicity of C, CN_x, BN_x, BC_x, and BC_xN_y nanostructures (nanotubes, nanofibers, nanoparticles, fullerenes, nanoribbons, etc.).[1]

In the last three decades, research on ternary boron carbonitride (BC_xN_y) solid solutions has received considerable attention, inspired by the promising combination of the excellent chemical, thermal and mechanical properties of the hexagonal and cubic allotropic forms of BN (*h*-BN, *c*-BN) and C (graphite, diamond). From the very beginning, special interest has been paid to the BC_xN stoichiometry, understood as a substitution of BN atomic pairs by isoelectronic CC pairs that satisfies the charge neutrality condition expected for a stable ternary compound. Since then, practically all the experimental works on the synthesis of boron carbonitride in bulk form have reported a ternary BC_xN composition, both for hexagonal crystalline powders prepared by chemical methods from different precursors[2] and for cubic phases obtained by high-temperature and high-pressure (HT/HP) techniques.[3] In contrast, the synthesis of BC_xN_y compounds in thin film form−usually by chemical or physical vapor deposition methods−often produces a broad range of compositions far from BC_xN.[4−6] One of the main obstacles in the formation of a ternary BC_xN layered compound is its strong sensitivity to the conditions of synthesis. Actually, several theoretical [7] and experimental[4,6,8,9] studies have pointed to the metastable character of BC_xN_y, a fact that is frequently translated into elemental and/or binary phase segregation. In the case of phase segregation at the nanometric scale, its detection becomes complicated, and it is necessary to resort to high-resolution techniques for the analysis of the structure.

In this sense, there exist at present an abundant number of characterization techniques to study the composition and bonding structure of thin film materials.[11] Among them, the progress of highly spatially resolved imaging technologies as transmission electron microscopy (TEM) has signified a major improvement in the study of nanometric structures, especially when coupled to electron energy loss spectroscopy (EELS). In this way, the bonding structure and the spatial distribution of each element can be assessed simultaneously at a nanometric level. This powerful method of combining imaging and spectrometry has been extensively used for the characterization of B−C−N nanomaterials,[12,13] and can unequivocally determine whether there is phase segregation and a heterogeneous distribution of the constituent elements or not.

*Corresponding author. E-mail: caretti@icmm.csic.es.

(1) Yap, Y. K. B−C−N Nanotubes and Related Nanostructures. In *Lecture Notes in Nanoscale Science and Technology*; Zhiming, M., Wang, A. W., Salamo, G., Kishimoto, N., Eds.; Springer Science+ Business Media: New York, 2009; Vol. *6*.
(2) Kawaguchi, M.; Kawashima, T.; Nakajima, T. *Chem. Mater.* **1996**, *8*, 1197–1201.
(3) (a) Solozhenko, V. L.; Andrault, D.; Fiquet, G.; Mezouar, M.; Rubie, D. C. *Appl. Phys. Lett.* **2001**, *78*, 1385–1387. (b) Langenhorst, F.; Solozhenko, V. L. *Phys. Chem. Chem. Phys.* **2002**, *4*, 5183–5188.
(4) (a) Ulrich, S.; Ehrhardt, H.; Theel, T.; Schwan, J.; Westermeyr, S.; Scheib, M.; Becker, P.; Oechsner, H.; Dollinger, G.; Bergmaier, A. *Diamond Relat. Mater.* **1998**, *7*, 839–844.
(5) (a) Gago, R.; Jiménez, I.; Albella, J. M. *Thin Solid Films* **2000**, *373*, 277–281. (b) Gago, R.; Jimenez, I.; Agullo-Rueda, F.; Albella, J. M.; Czigany, Z.; Hultman, L. *J. Appl. Phys.* **2002**, *92*, 5177–5182.
(6) (a) Linss, V.; Barzola-Quiquia, J.; Häussler, P.; Richter, F. *Thin Solid Films* **2004**, *467*, 66–75.
(7) (a) Yuge, K. *Phys. Rev. B* **2009**, *79*, 144109 (6 pp.). (b) Lambrecht, W. R. L.; Segall, B. *Phys. Rev. B* **1993**, *47*, 9289–9296. (c) Zhang, R. Q.; Chan, K. S.; Cheung, H. F.; Lee, S. T. *Appl. Phys. Lett.* **1999**, *75*, 2259–2261.
(8) (a) Ulrich, S.; Kratzsch, A.; Leiste, H.; Stuber, M.; Schlossmacher, P.; Holleck, H.; Binder, J.; Schild, D.; Westermeyer, S.; Becker, P.; Oechsner, H. *Surf. Coat. Technol.* **1999**, *116*, 742–750.
(9) (a) Sauter, D.; Weinmann, M.; Berger, F.; Lamparter, P.; Muller, K.; Aldinger, F. *Chem. Mater.* **2002**, *14*, 2859–2870. (b) Linss, V.; Rodil, S. E.; Reinke, P.; Garnier, M. G.; Oelhafen, P.; Kreissig, U.; Richter, F. *Thin Solid Films* **2004**, *467*, 76–87. (c) Krause, M.; Bedel, L.; Taupeau, A.; Kreissig, U.; Munnik, F.; Abrasonis, G.; Kolitsch, A.; Radnoczi, G.; Czigany, Z.; Vanhulsel, A. *Thin Solid Films* **2009**, *518*, 77–83.
(10) Hellgren, N.; Berlind, T.; Gueorguiev, G. K.; Johansson, M. P.; Stafstrom, S.; Hultman, L. *Mater. Sci. Eng., B* **2004**, *113*, 242–247.
(11) H.Bubert, H. J. *Surface and Thin Film Analysis: A Compendium of Principles, Instrumentation, and Applications*; Wiley-VCH: Weinheim, Germany, 2002.
(12) (a) Suenaga, K.; Colliex, C.; Demoncy, N.; Loiseau, A.; Pascard, H.; Willaime, F. *Science* **1997**, *278*, 653–655. (b) Zhang, Y.; Suenga, K.; Colliex, C.; Lijima, S. *Science* **1998**, *281*, 973–975. (c) Johansson, M. P.; Suenaga, K.; Hellgren, N.; Colliex, C.; Sundgren, J.-E.; Hultman, L. *Appl. Phys. Lett.* **2006**, *76*, 825–827.
(13) (a) Vinu, A.; Terrones, M.; Golberg, D.; Hishita, S.; Ariga, K.; Mori, T. *Chem. Mater.* **2005**, *17*, 5887–5890. (b) Wang, W. L.; Bai, X. D.; Liu, K. H.; Xu, Z.; Golberg, D.; Bando, Y.; Wang, E. G. *J. Am. Chem. Soc.* **2006**, *128*, 6530–6531. (c) Enouz, S.; Stephan, O.; Cochon, J. L.; Colliex, C.; Loiseau, A. *Nano Lett.* **2007**, *7*, 1856–1862. (d) Kim, S. Y.; Park, J.; Choi, H. C.; Ahn, J. P.; Hou, J. Q.; Kang, H. S. *J. Am. Chem. Soc.* **2007**, *129*, 1705–1716. (e) Enouz-Vedrenne, S.; Stephan, O.; Glerup, M.; Cochon, J. L.; Colliex, C.; Loiseau, A. *J. Phys. Chem. C* **2008**, *112*, 16422–16430.

Published on Web 03/01/2010

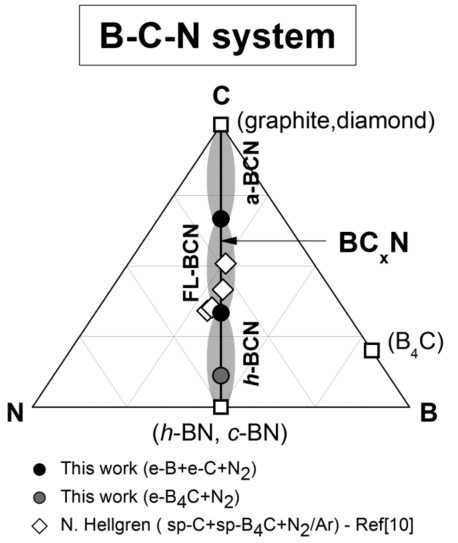

Figure 1. Ternary B−C−N compositional diagram, displaying some of the more characteristic compounds (white squares). The BC_xN samples studied in this work (black and gray dots), and the corresponding structural transitions, are shown together with the fullerene-like (FL) BC_xN samples reported in ref 10 (diamond-shaped dots).

Therefore, in this communication, we present a TEM & EELS study of the atomic structure of BC_xN coatings grown on silicon wafers by ion beam assisted deposition (IBAD) at room temperature, without intentional heating of the substrate. We have determined how the structure of graphitic-like BC_xN compounds is affected by the incorporation of C by examining samples with $BC_{0.25}N$, BCN and BC_4N stoichiometry (see the Supporting Information). This investigation is of special interest in the frame of potential properties and applications expected for the BC_xN compositional line as a function of the C content. For instance, the energy gap of *h*-BC_xN can be tuned through C concentration, exhibiting an electronic behavior that varies from a wide band gap insulator (*h*-BN) to a semimetal (graphite).[14] In accordance, graphitic BC_2N semiconductors have been predicted theoretically[15] and obtained using different methods.[16,17] Furthermore, we reported an improvement of the mechanical and tribological properties with the incorporation of C in *h*-BC_xN coatings,[18] with the best performance found for a BC_4N amorphous film.[19]

Figure 2 shows the 30×30 nm^2 TEM micrographs obtained for $BC_{0.25}N$, BCN and BC_4N compositions. For low C content, the laminar atomic distribution of *h*-BN is preserved in boron carbonitride compounds, as confirmed by the characteristic (001) basal planes observed

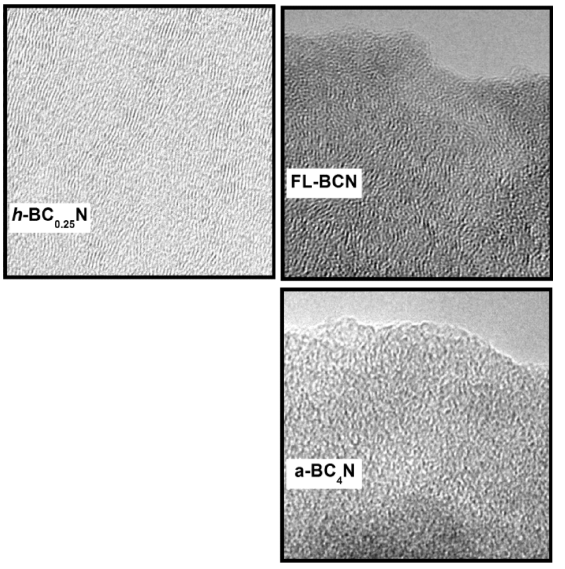

Figure 2. TEM micrographs (30×30 nm^2) obtained for *h*-$BC_{0.25}N$, FL-BCN, and a-BC_4N samples.

in the TEM picture of $BC_{0.25}N$. It should be noted that these basal planes are preferentially oriented perpendicular to the substrate surface. However, by increasing the C content toward a BCN stoichiometry, it is clear that the hexagonal stacking sequence typical of *h*-BN transforms into a fullerene-like (FL) structure consisting of cross-linked curved planes. In this case, there is a partial breakdown of the preferential orientation due to the curvature. Similarly structured FL-BC_xN_y thin films have been also synthesized by Hellgren et al.[10] for a wide range of compositions, including the BC_xN stoichiometry under study in this communication. Specifically, FL-BC_xN ($1 < x < 2$) thin films with interesting elastic properties were grown by cosputtering of C and B_4C in a mixed N_2/Ar discharge, as indicated in the ternary B−C−N diagram of Figure 1. Finally, regarding the BC_4N composition, the sample shows an amorphous structure, i.e., no structural order is evident by TEM.

Altogether, the micrographs of Figure 2 reveal significant changes in the atomic structure of the BC_xN thin films grown by IBAD as we increase the C concentration. When C is the minority element in the material, a planar stacking geometry resembling the original *h*-BN structure is still present. As C content is raised, faults or defects formed by the inclusion of C atoms in the hexagonal structure give rise to nonsix-membered rings, which are known to be responsible for the basal-plane curving and the creation of the observed FL structure. When C is majoritary, the amorphization of the compound is induced by C atoms incorporation. As summarized in the ternary diagram of Figure 1, these observations imply that, for B−C−N compounds grown by IBAD, there is a limiting C concentration of ~30 at % for which C can be assimilated as part of the *h*-BN structure without breaking the hexagonal symmetry. For higher C concentrations up to a ~65 at %, a dominant amorphization of the material occurs. The transition from a hexagonal to a fully

(14) Watanabe, M.; Mizushima, K.; Itoh, S.; Mashita, M. Semiconductor device using semiconductor BCN compounds. U.S. Patent 5 747 118, April 20, **1999**.
(15) Liu, A. Y.; Wentzcovitch, R. M.; Cohen, M. L. *Phys. Rev. B* **1989**, *39*, 1760–1765.
(16) Watanabe, M. O.; Itoh, S.; Mizushima, K.; Sasaki, T. *J. Appl. Phys.* **1995**, *78*, 2880–2882.
(17) Yao, B.; Chen, W. J.; Liu, L.; Ding, B. Z.; Su, W. H. *J. Appl. Phys.* **1998**, *84*, 1412–1415.
(18) Caretti, I.; Jimenez, I.; Gago, R.; Caceres, D.; Abendroth, B.; Albella, J. M. *Diamond Relat. Mater.* **2004**, *13*, 1532–1537.
(19) Caretti, I.; Albella, J. M.; Jimenez, I. *Diamond Relat. Mater.* **2007**, *16*, 63–73.

amorphous BC_xN material occurs within the $1 < x < 4$ range through an intermediate FL structure.

The described amorphization with increasing C is consistent with the fact that stoichiometric *h*-BN grown by IBAD generally displays a hexagonal or turbostratic structure whereas evaporated C films are commonly highly amorphous. Notice that the interaction between hexagonal sheets is stronger in *h*-BN than graphite because of the partial ioinic character of B−N bonds compared to covalent C−C bonds. Moreover, the impinging 500 eV N_2^+ ions transfer a much higher energy to the depositing atoms than the evaporated C atoms, whose kinetic energy is ~0.3 eV. Hence, under this growing conditions, C will most likely contribute to the formation of highly disordered phases when it is the predominant element during the synthesis of BC_xN layers.

The bonding structure of BCN and BC_4N compounds was investigated by EELS (see the Supporting Information). No oxygen intensity is detected at the O(1s) edge in any of the EELS spectra. The B(1s), C(1s), and N(1s) edges do not exhibit significant changes in the bonding structure of BCN and BC_4N, mainly because of the low spectral resolution of the electron analyzer (~1 eV). Nevertheless, attending to the π^*/σ^* ratio of each element, some interesting conclusions can be extracted. Clearly, the C(1s) π^* intensity of BC_4N has decreased compared to that of BCN, whereas the B(1s) and N(1s) π^* intensities remain approximately the same. This trend can be interpreted as a reduction of relative amount of sp^2-bonded C atoms in the material, the sp^2 content being the same in the case of B and N atoms. In the highly disordered BC_4N amorphous phase, the trigonal planar bonding symmetry of sp^2 C atoms is significantly reduced in comparison with the hexagonal or FL structures, which consist mainly of flat or curved B−C−N planes, respectively. Therefore, when grown by IBAD, an increase in the number of bulky 4-fold coordinated sp^3 C atoms is expected in the amorphous phase. Similarly, an increase in the sp^3 content has also been detected by XANES with increasing C concentration.[18]

The fact that unlike C, the sp^2-related π^* intensity of B and N is barely changed from BCN to BC_4N, shows that these atoms maintain their hexagonal character disregard for the C concentration. This means that sp^3 C sites are located at the grain boundaries of hexagonal BN and BCN domains or that segregation of amorphous C occurs. However, neither the TEM micrograph of Figure 2 nor the energy-filtered TEM (EFTEM) elemental maps obtained by the three-windows method support the hypothesis of phase segregation. Figure 3 displays the zoomed-out TEM image (top left panel) of the amorphous BC_4N sample shown in Figure 2, and the respective EFTEM images for B, C, and N. The latter were taken by selecting the corresponding energy range for the different B, C and N species in the electron detector. Notice that the three-windows method works only in areas where the specimen is thin enough, i.e., of the order of the mean free path of plasmon losses. Accordingly, the thickest areas (i.e., dark areas) in the a-BC_4N TEM image of Figure 3 are not suitable to elemental mapping. Therefore, the elemental distribution has to be checked out in the thin areas close to the edge of the sample. Attending to each EFTEM image, it can be seen that every atom type is homogeneously distributed all along the sample, and no differences in contrast are observed further than the elemental sensitivity of the different atoms.

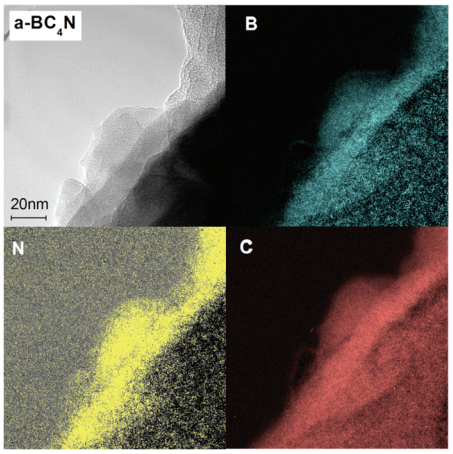

Figure 3. Energy-filtered TEM images of the a-BC_4N compound showing a homogeneous distribution of boron, carbon, and nitrogen elements all along the amorphous material.

In agreement with previous studies by XANES,[19] EFTEM mapping confirms the absence of segregation in the material and the formation of a ternary solid solution with amorphous structure (a-BC_4N) at the scale of ~1 nm, which is the spatial resolution that can be achieved by EFTEM mapping. This is an important result that demonstrates the possibility of synthesizing ternary B−C−N materials by IBAD, even for a high C content, in contrast with often reported phase segregation.[6,9,12]

In conclusion, the structure of the BC_xN compounds grown by IBAD has shown to be quite sensitive to the C concentration, as expected for compounds with supposedly different mechanical and electronic properties. The structure varies from a hexagonal laminar phase when $x < 1$ to a fully amorphous compound for $x \geq 4$. For $x = 1$, the compound consists of curved hexagonal planes in the form of a fullerene-like structure, being an intermediate structure in the process of amorphization due to C incorporation. No segregation was observed in the BC_xN materials studied in this communication, which indicates the formation of ternary compounds by IBAD.

Acknowledgment. This work has been partially financed by the EU-sixth Framework Program, Project FOREMOST, under Contract NMP3-CT-2005-515840. We also acknowledge the Spanish MICINN for support through project Consolider FUNCOAT CSD2008-0023.

Supporting Information Available: Experimental details and EEL spectra (PDF). This material is available free of charge via the Internet at http://pubs.acs.org.